REPORT DOCUMENTATION PAGE

Form Approved OMB No. 0704-0188

Public reporting burden for this collection of information is estimated to average 1 hour per response, including the time for reviewing instructions, searching existing data sources, gathering and maintaining the data needed, and completing and reviewing this collection of information. Send comments regarding this burden estimate or any other aspect of this collection of information, including suggestions for reducing this burden to Department of Defense, Washington Headquarters Services, Directorate for Information Operations and Reports (0704-0188), 1215 Jefferson Davis Highway, Suite 1204, Arlington, VA 22202-4302. Respondents should be aware that notwithstanding any other provision of law, no person shall be subject to any penalty for failing to comply with a collection of information if it does not display a currently valid OMB control number. PLEASE DO NOT RETURN YOUR FORM TO THE ABOVE ADDRESS.

1. REPORT DATE (DD-MM-YYYY) 11-05-2004	REPRINT	
4. TITLE AND SUBTITLE Water Vapor Retrieval Using	g the FLAASH Atmospheric Correction	5a. CONTRACT NUMBER
Algorithm		5b. GRANT NUMBER
	•	5c. PROGRAM ELEMENT NUMBER 61102F
6.AUTHOR(S) G.W. Felde, G.P. Anderson,	J.A. Gardner, S.M. Adler-Golden*,	5d. PROJECT NUMBER 1010
M.W. Matthews* and A. Beck		5e. TASK NUMBER HS
	·	5f. WORK UNIT NUMBER A1
7. PERFORMING ORGANIZATION NAME(S	S) AND ADDRESS(ES)	8. PERFORMING ORGANIZATION REPORT

7. PERFORMING ORGANIZATION NAME(S) AND ADDRESS(ES)

Air Force Research Laboratory/VSBYH 29 Randolph Road Hanscom AFB MA 01731-3010

20040518 082

9. SPONSORING / MONITORING AGENCY NAME(S) AND ADDRESS(ES)

10. SPONSOR/MONITOR'S ACRONYM(S) AFRL/VSBYH

11. SPONSOR/MONITOR'S REPORT **NUMBER(S)**

AFRL-VS-HA-TR-2004-1071

12. DISTRIBUTION / AVAILABILITY STATEMENT

Approved for Public Release; Distribution Unlimited.

*SSI, Burlington, MA

13. SUPPLEMENTARY NOTES

REPRINTED FROM: PROCEEDINGS OF THE SPIE DEFENSE AND SECURITY SYMPOSIUM, Orlando, FL, 12-16 April 2004.

FLAASH (Fast Line-of-sight Atmospheric Analysis of Spectral Hypercubes) is a first-principles atmospheric correction algorithm for visible to shortwave infrared (SWIR) hyperspectral data. The first is retrieval of atmospheric parameters, visibility (which is related to the aerosol type and distribution) and column water vapor. The second step is solving the radiation transport equation for the given aerosol and column water and transformation to surface reflectance. The focus of this paper is on the FLAASH water vapor retrieval algorithm. Modeled radiance values in the spectral region of one water vapor absorption feature are calculated from MODTRAN 4 using several different water vapor amounts and are using to generate a Look-Up Table (LUT). The water band typically used is 1030 nm but either the 940 and 820 nm band may also be used. Measured radiation values are compared to the LUT to determine the column water vapor amount for each pixel in the scene. We compare the results of water retrievals for each of these bands and also the results of their corresponding reflectance retrievals.

15. SUBJECT TERMS Hyperspectral			ric correction		
16. SECURITY CLAS	SIFICATION OF:		17. LIMITATION OF ABSTRACT	18. NUMBER OF PAGES	19a. NAME OF RESPONSIBLE PERSON Gerald Felde
a. REPORT UNCLAS	UNCLAS	c. THIS PAGE UNCLAS	SAR	11	19b. TELEPHONE NUMBER (include area code) 781-377-3136

Water vapor retrieval using the FLAASH atmospheric correction algorithm

Gerald W. Felde^{*a}, Gail P. Anderson^a, James A. Gardner^a, Steven M. Adler-Golden^b, Michael W. Matthew^b, and Alexander Berk^b
^aAir Force Research Laboratory, Space Vehicles Directorate, 29 Randolph Rd., Hanscom AFB, MA 01731;
^bSpectral Sciences, Inc., 4 Fourth Ave., Burlington, MA 1803

ABSTRACT

FLAASH (Fast Line-of-sight Atmospheric Analysis of Spectral Hypercubes) is a first-principles atmospheric correction algorithm for visible to shortwave infrared (SWIR) hyperspectral data. The algorithm consists of two main steps. The first is retrieval of atmospheric parameters, visibility (which is related to the aerosol type and distribution) and column water vapor. The second step is solving the radiation transport equation for the given aerosol and column water and transformation to surface reflectance. The focus of this paper is on the FLAASH water vapor retrieval algorithm. Modeled radiance values in the spectral region of one water vapor absorption feature are calculated from MODTRAN 4 using several different water vapor amounts and are used to generate a Look-Up Table (LUT). The water band typically used is 1130 nm but either the 940 or 820 nm band may also be used. Measured radiance values are compared to the LUT to determine the column water vapor amount for each pixel in the scene. We compare the results of water retrievals for each of these bands and also the results of their corresponding reflectance retrievals.

Keywords: hyperspectral, atmospheric correction, water vapor retrieval, FLAASH

1. INTRODUCTION

The Fast Line-of-sight Atmospheric Analysis of Spectral Hypercubes (FLAASH) atmospheric correction algorithm/code is a software package developed by the Air Force Research Laboratory, Space Vehicles Directorate (AFRL/VS), Hanscom AFB and Spectral Sciences, Inc. (SSI) to support the analyses of visible to shortwave infrared (Vis - SWIR) hyperspectral and multispectral imaging sensors. The algorithm derives its first-principles physics-based calculations from the MODTRAN4 (Berk et al., 1996; Anderson et al., 2000) radiative transfer code. The main objective of FLAASH is to eliminate atmospheric effects caused by molecular and particulate scattering and absorption from the 'radiance-at-detector' measurements in order to retrieve 'reflectance-at-surface' values. In order to achieve this objective, FLAASH employs two main steps. The first is retrieval of atmospheric parameters, visibility (which is related to the aerosol type and distribution) and column water vapor. Since current methods allow aerosol retrieval over a very limited set of surface types (dark land pixels), only an average visibility is obtained for a scene. On the other hand, the spectral signature of water vapor is sufficiently distinct that the column amount may be retrieved on a pixel-by-pixel basis. The second step is solving the radiation transport equation for the given aerosol and column water and transformation to surface reflectance. The emphasis of this paper is on the application of the FLAASH water vapor determination algorithm and subsequent retrieval of surface reflectance spectra using AVIRIS hyperspectral radiance measurements as the input.

^{*}Gerald.Felde@hanscom.af.mil; phone 781-377-3136; fax 781-377-3138

2. DESCRIPTION OF FLAASH

MODTRAN calculated spectral radiance outputs are central to FLAASH operation. The MODTRAN calculations use the viewing and solar angles and the mean surface elevation of the measured scene. In addition, selection of reasonable MODTRAN standard atmosphere and aerosol models should be made. The outputs from MODTRAN are convolved with the sensor filter functions so that the radiance simulations have the same spectral characteristics (i.e., channel center wavelengths and FWHMs) as the measurements. A typical FLAASH run contains three sets of MODTRAN calculations. The first set is required for the preliminary column water retrieval of each pixel in the scene. A user estimate of the scene visibility is an additional input needed for this set. The mean value of the retrieved column water is used as input to the second set, which is required for the scene average visibility retrieval. This visibility value is used as input to the third set, which is used for the final column water vapor determination and reflectance spectra retrieval of each pixel in the scene. For the water column and visibility MODTRAN calculations. the parameter of interest (for visibility it is actually inverse visibility) is varied in even steps over the likely range of values in the cube. The ground albedo is also varied over the values of 0, 0.5, and 1, so there are two nested loops. The spectral range of each set of MODTRAN calculations must contain the wavelengths required for the task at hand - the relevant water bands for the preliminary water column determination, the bands required for the visibility determination, and the full range of the instrument for the final water column determination and reflectance spectra retrieval.

FLAASH processes radiance images with spectral coverage from wavelengths in the solar reflective regime where thermal emission can be neglected. For this situation the spectral radiance L* at a sensor pixel may be parameterized as (Vermote et al., 1994, Staenz et al., 1996, Adler-Golden et al., 1998, Matthew et al., 2000)

$$L^* = A\rho/(1-\rho_e S) + B\rho_e/(1-\rho_e S) + L^*_a$$
 (1)

where ρ is the pixel surface reflectance, ρ_e is an average surface reflectance for the surrounding region, S is the spherical albedo of the atmosphere (capturing the backscattered surface-reflected photons), L*a is the radiance backscattered by the atmosphere without reaching the surface, and A and B are surface independent coefficients that vary with atmospheric and geometric conditions. The spatially averaged reflectance, ρ_e , is used to account for "adjacency effects", i.e., radiance contributions that, because of atmospheric scattering, originate from parts of the surface not in the direct line of sight between sensor and targeted pixel. All of the variables are implicitly wavelength dependent. The first term in Equation (1) corresponds to the radiance reaching the surface (from both sky-shine and direct solar illumination) that is backscattered directly into the sensor, while the second term corresponds to the radiance from the surface that is re-scattered by the atmosphere into the sensor.

After the atmospheric retrievals of visibility and column water vapor (discussed later) are performed, Equation (1) is solved for the pixel surface reflectances in all of the sensor channels. The solution is based on a method in which the spatially averaged radiance image L^*_e is used to estimate the averaged reflectance ρ_e . This is done using an approximate equation derived from Equation (1):

$$L_{e}^{*} = (A+B)\rho_{e}/(1-\rho_{e}S) + L_{a}^{*}$$
(2)

As in Equation (1), the variables are all wavelength (or equivalently, channel) dependent. L*_e is obtained from the measured radiance values, L*, by spatial averaging of the data using a point-spread function that describes the atmospheric scattering of ground reflected photons into the sensor pixel. The spatial averaging excludes the measured values for cloud-filled pixels because clouds do not contribute to the near-surface pixel cross-talk. These pixels are replaced by the scene average radiance of all cloud-free pixels.

The cloudy pixels are found using a combination of brightness, color balance, and column water vapor tests (Ackerman et al., 1998 and Borel et al., 1999). Starting from the known L_e^* for each pixel and the coefficients A, B, S and L_a^* (which are extracted from the MODTRAN radiance simulations), Equation (2) is solved for ρ_e . The result is inserted into Equation (1), which is then solved for the reflectance ρ .

There is a final optional step available in FLAASH that can be applied to the retrieved reflectance cube. It is called spectral polishing, a term coined by Boardman (1998) to describe a mathematical renormalization method for removing artifacts from reflectance spectra using only the data itself. When properly implemented, polishing dramatically reduces spurious, systematic spectral structure due to wavelength registration errors and molecular absorption residuals while leaving true spectral features of the surface intact. It is important to note that FLAASH has an automated wavelength recalibration algorithm, which can also be used to improve the retrieved reflectance spectra. This algorithm uses atmospheric molecular absorption features (e.g., oxygen, carbon dioxide, water vapor) to quantify wavelength error by fitting an absorption band shape in the measured radiance spectra to MODTRAN model calculations (Felde et al., 2003). If the wavelength recalibration option is selected, it is implemented in the FLAASH processing flow immediately after the preliminary water vapor retrieval.

The visibility or aerosol overburden (optical column, not vertical structure) is currently addressed through a general reflectance ratio-based algorithm, retrieving only the scene-average aerosol amount. The algorithm is based on the empirical observation by Kaufman et al. (1997) that for natural dark terrain (primarily vegetation) the reflectances at certain wavelengths, such as 660 nm and 2100 nm, are in nearly a fixed ratio (for these wavelengths, the ratio is ~0.45). The Equation (1) and (2) calculations are iterated over a range of visibility values using the appropriate set of MODTRAN radiance simulations (discussed above). For each visibility, the scene-average 660 nm and 2100 nm reflectances for the dark pixels are retrieved, and the "best" estimate of visibility is interpolated by matching the ratio to 0.45.

3. COLUMN WATER VAPOR RETRIEVAL ALGORITHM

Water vapor provides the strongest molecular absorption features in the visible to SWIR range. In fact, water vapor absorption is so strong in the vicinity of 1400 and 1900 nm that the atmosphere is opaque and thus it is physically impossible to retrieve water vapor and surface reflectance in these wavelength regions. Water vapor absorption is also centered near 820, 940, and 1130 nm. However, at these wavelengths, the atmosphere is typically not opaque and so water and surface reflectance retrieval is possible.

The physical basis of the FLAASH water vapor retrieval algorithm is illustrated in Fig. 1. This figure shows the effect of varying amounts of column water vapor (0, 2000, 4000, ... 10000 atm-cm) on the radiance spectra in the vicinity of the 820, 940, and 1130 nm water absorption regions. The absorption "valleys" get deeper with increasing amounts of water vapor. These radiance spectra were generated from 5 cm⁻¹ resolution MODTRAN calculations, which were convolved to correspond to the AVIRIS channel center wavelengths and FWHMs. The AVIRIS channel center wavelengths are ~10 nm apart and the FWHMs are also ~10nm. The MODTRAN calculations used the viewing and solar conditions (56 degree solar zenith angle) corresponding to an AVIRIS radiance data cube for Fort A.P. Hill, VA, which was analyzed with FLAASH (this analysis is discussed later). Also, the calculations used a surface albedo of 0.5, the FLAASH retrieved scene-average visibility of 33 km, the rural aerosol model, the Isaacs 2-stream multiscatter model, and the tropical atmospheric profiles. Eleven sets of MODTRAN calculations were done, keeping all parameters constant, except for scaling the tropical moisture profile to correspond to column water values of 0, 1000, 2000, ... 10000 atm-cm. (It should be noted that the 0 atm-cm simulation actually was based on a scale factor of 0.01 and thus in reality used a moisture profile containing 51 atmcm column water vapor. This is why the curve labeled 0 water in Fig. 1 has small valleys near 820, 940, and 1130 nm. The curve for an exact value of 0 water would not have these small valleys.) For clarity, only six of the resulting eleven simulated radiance spectra were plotted in Fig. 1. There are six model atmospheres available in MODTRAN (Table 1) and their column water vapor values range from ~ 500 to 5000 atm-cm. In the Fig. 1 MODTRAN radiance simulations, the maximum water value used was twice that of the typical tropical moisture profile available in MODTRAN. This was done to account for extremely moist atmospheres, which can occur in nature.

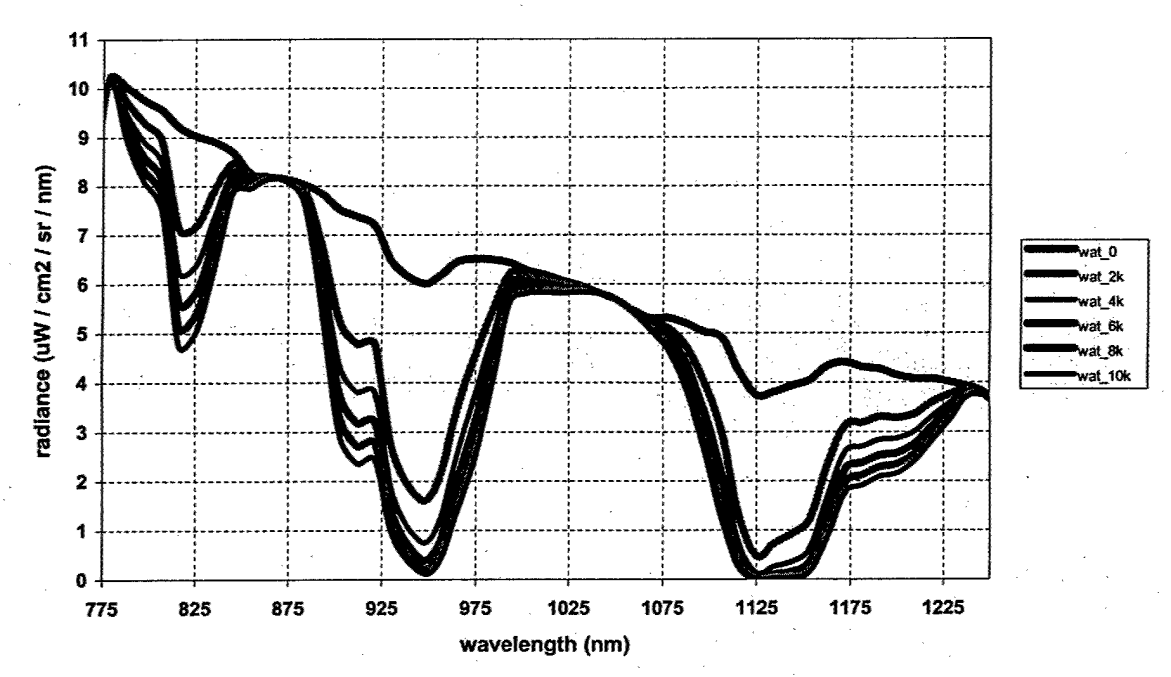


Fig. 1. MODTRAN simulated radiance spectra for varying amounts of column water vapor.

Table 1. Column Water Vapor Values of MODTRAN's Atmospheric Models.

Atmospheric Model	Column Water Vapor (atm-cm)		
sub-arctic winter	518		
mid-latitude winter	1060		
U.S. standard	1762		
sub-arctic summer	2589		
mid-latitude summer	3636		
tropical	5119		

In order to quantify and compare the sensitivity to water vapor in the 820, 940, and 1130 nm regions using the simulated radiance spectra, the depth of each absorption valley for each column water vapor amount was computed. This was done by dividing each absorption band minimum radiance value by the zero water radiance value at the same wavelength. The resulting values were multiplied by 100 in order to transform them into percentages. The final results are plotted in Fig. 2. There are three curves of depth of absorption valley vs. column water vapor – one for each of the three absorption regions. It should be noted that the greater the depth, the smaller the value on the vertical axis. For the column water vapor range of 0 to ~ 4000 atm-cm, the 940 and 1130 nm curves are similar. Both show a rapid increase in valley depth with increasing water vapor, which indicates a strong sensitivity to water vapor. On the other hand, for this same water range, the 820 nm curve shows a much more gradual increase in valley depth with increasing water, which indicates a much weaker sensitivity to water. For water vapor values greater than 4000 atm-cm, the magnitude of the slopes of all three curves is small compared to their respective slopes for water values less than 4000 atm-cm. This indicates less sensitivity to water vapor in all three absorption regions for water

vapor values greater than 4000 atm-cm. The difference between the 4000 and 7000 atm-cm percent radiance values are 9.10, 8.40, and 3.90 for the 820, 940, and 1130 nm curves, respectively. This indicates similar sensitivity to water vapor at 820 and 940 nm for this range of vapor values but weaker sensitivity at 1130 nm. The difference between the 7000 and 10000 atm-cm percent radiance values are 6.48, 3.41, and 0.87 for the 820, 940, and 1130 nm curves, respectively. Thus the greatest sensitivity to water vapor for this water range is at 820 nm. At 1130 nm, the radiance values are nearly zero for this water range, which indicates that the atmosphere is essentially opaque and thus has no sensitivity to water vapor. The above discussion points out that either the 1130 or 940 nm water vapor band is the best choice for water retrieval for non-tropical moisture conditions (recall that the tropical moisture profile in MODTRAN has a column water vapor value of 5119 atm-cm, see Table 1) and that either the 940 or 820 nm band is the best choice for retrieval under very moist conditions.

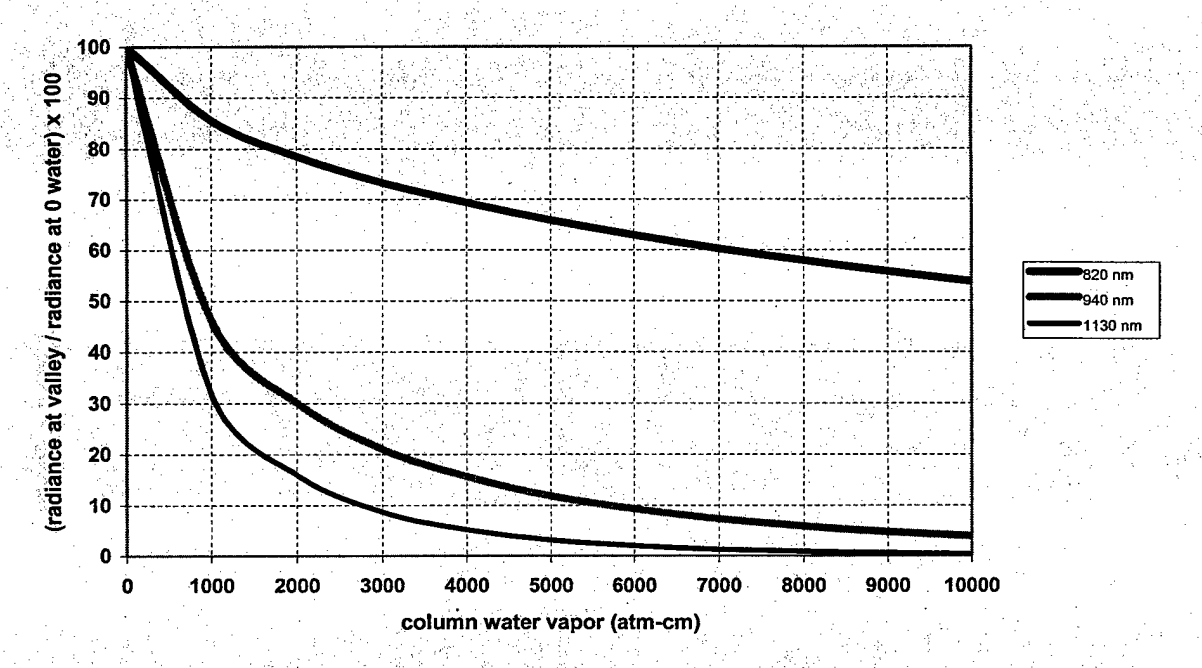


Fig. 2. Absorption valley depths for three water vapor bands as a function of column water vapor amount.

The principal component of the FLAASH column water vapor retrieval algorithm is the strong dependence/correlation of water vapor column amount to the ratio of 'reference' (the shoulders of the water absorption band) and 'absorption' (center of the same absorption band) radiances. The retrieved water vapor also depends somewhat on the absolute values of these radiances, which vary most directly with the surface reflectance. This dependence arises because the amount of water absorption in the atmospherically-scattered and surface-reflected radiance components is slightly different; the absorption is generally smaller for the atmospherically scattered photons, which avoid the high concentration of water vapor close to the ground. A Look-Up Table (LUT) is then built around these dependencies.

The FLAASH column water vapor retrieval algorithm uses Equation (1) but for simplicity ignores the adjacency effect, replacing ρ_e with ρ . This is a good approximation because the wavelengths required for water retrieval are fairly long and thus atmospheric scattering is minimal. The MODTRAN generated A, B, S, and L*a coefficients extracted for each channel and column water amount are used to simulate a set of absorption and reference radiances, L*. This is done for an even grid of surface reflectance values from 0 to 1, inclusive, spaced 0.01 apart. The ratio of the reference to absorption bands is computed for each grid point. The result is a set of triples, consisting of {column water vapor, reference radiance, ratio} that span both the entire expected range of water column and surface reflectances. These values are initially evenly

spaced in the dependent variable to be retrieved (water vapor) but not in the independent variables (measured radiance – reference and ratio).

The triples are transformed into an even grid in reference radiance and ratio. The resulting 2-dimensional LUT has reference radiance and ratio as independent variables and the water vapor as the dependent variable. This LUT allows a direct table look-up of water column, given measured reference radiance and ratio, and thus it is searched to retrieve the column water vapor value for each pixel. In occasional instances, the reference radiance or ratio value may lie outside the LUT. In such cases the pixel is flagged to denote LUT failure, and the water vapor for that pixel is then assigned the average of the valid retrievals for the scene. The water determination is a necessary precursor to the final reflectance retrieval of each individual pixel because it permits calculation of the correct values for the coefficients in Equations (2) and (1).

4. FLAASH WATER AND REFLECTANCE RETRIEVAL RESULTS

Three cloud-free AVIRIS radiance data cubes collected under substantially different atmospheric moisture conditions were selected for analysis with FLAASH: (1) Fort Huachuca, AZ on 12 November 1999, (2) Fort A.P. Hill, VA on 8 November 1999, and (3) Camp Ripley, MN on 10 August 2000. For each radiance data cube, three different column water vapor retrievals were performed, using the 1130, 940, and 820 nm absorption features, respectively. Also, three different reflectance cubes were retrieved from each radiance cube using the 1130, 940, and 820 nm water results, respectively. The following FLAASH options were employed: automated wavelength recalibration, adjacency correction, and spectral polishing.

The water vapor column retrieval results for these three cubes are given in Table 2. Invalid pixels are those whose water reference radiance or ratio (of reference radiance to absorption radiance) value lie outside the LUT and thus retrieval of water vapor was not possible. The majority of invalid pixels are typically those containing surface water (e.g., lakes). Often it is not possible to determine water vapor over surface water because of its near zero radiance values at the wavelengths corresponding to the water vapor absorption features, which is a result of the very small reflectance of liquid water in this spectral region. The Fort Huachuca and Camp Ripley scenes both contain no invalid pixels, which is consistent with the fact that there is no surface water in these scenes. On the other hand, the ~ 1 % invalid pixels for the Fort A.P. Hill cube corresponds to it having ~1 % surface water pixels in the scene. The average retrieved column water vapor value obtained from using a particular band for Camp Ripley is ~ 2 times that for Fort A.P. Hill, and the water value for each band for Fort A.P. Hill is ~ 2.5 times that for Fort Huachuca. For each scene, the average retrieved water vapor values are similar for the 1130 and 940 nm absorption bands, but are considerably larger for the 820 nm band. This is consistent with the observations obtained from Figs. 1 and 2 that for atmospheres containing less than ~ 4000 atm-cm column water vapor, the water vapor column sensitivity is much stronger for the 1130 and 940 nm absorption bands compared to the sensitivity for the 820 nm band. Also, this suggests that the retrieved water values obtained from either the 1130 or 940 nm region should be much closer to the true value than the retrieved value obtained from the 820 nm region. This hypothesis was verified by comparison of individual pixel reflectance spectra for each scene from the three different reflectance cubes, which were retrieved from each radiance cube using the 1130, 940, and 820 nm water results, respectively. The comparisons showed that some residual water vapor signal was evident in the reflectance spectra obtained with the 820 nm water results but not in the reflectance spectra obtained with the other two bands.

Examples of some reflectance spectra comparisons for two pixels from the Fort A.P. Hill scene are given in Figs. 3 and 4. Fig. 3 is a building pixel and Fig. 4 is a grass pixel. The retrieved column water vapor amounts for each of these individual pixels were almost exactly the same as the scene average values listed in Table 2. The reflectance spectra obtained using the 1130 and 940 nm regions for water determination for each of these two pixels was essentially identical because the water values were nearly the same. Thus, a single curve is used in each figure for these two spectra. The FLAASH reflectance spectra using the 1130 or 940 nm water vapor retrievals are good, i.e., no spikes or valleys at 820, 940, or

1130 nm. On the other hand, the reflectance spectra using the 820 nm water vapor retrievals contain noticeable over-correction (i.e., spikes) at 940 and 1130 nm, and also on the wings of the two opaque absorption regions, which are centered near 1400 and 1900 nm. This indicates that the amount of water retrieved using the 820 nm absorption feature was too large. It should be noted that there is no spike on this curve at 820 nm. The 820 nm absorption feature is considerably weaker than either the 940 or 1130 feature (see Fig. 1). Apparently, the 17 % larger water vapor value obtained from the 820 nm absorption isn't enough of a difference to adversely affect the the reflectance retrieval in the 820 nm region.

Table 2. FLAASH Water Vapor Column Retrieval Results.

Location	Water Vapor Absorption Feature Used	Average Water Vapor (atm-cm)	Standard Deviation	Percent Invalid Pixels
	and the constraint of the constraint			
Ft. Huachuca	1130 nm	588	28	0
	940 nm	573	44	0
	820 nm	711	35	0
Ft. A.P. Hill	1130 nm	1516	136	1.06
,	940 nm	1505	179	1.18
	820 nm	1763	147	1.07
Camp Ripley	1130 nm	2904	177	0
	940 nm	3206	185	0
	820 nm	3849	111	0

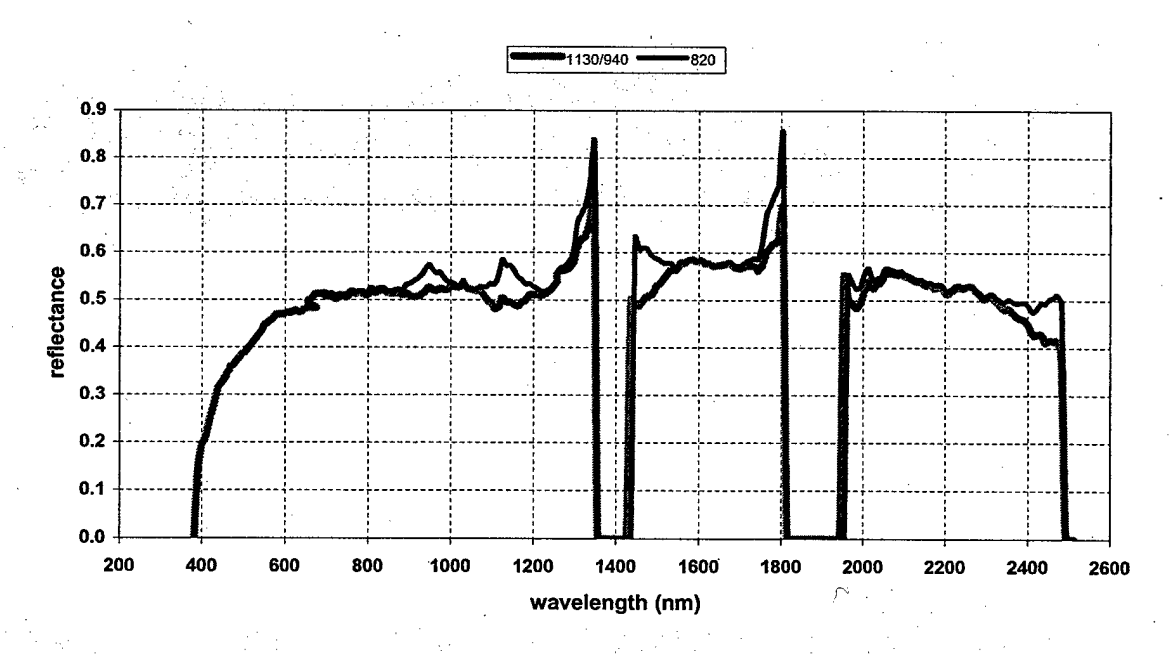


Fig. 3. Building reflectance spectra retrieved by FLAASH using the 1130 (or 940) and 820 nm regions for water vapor column determination.

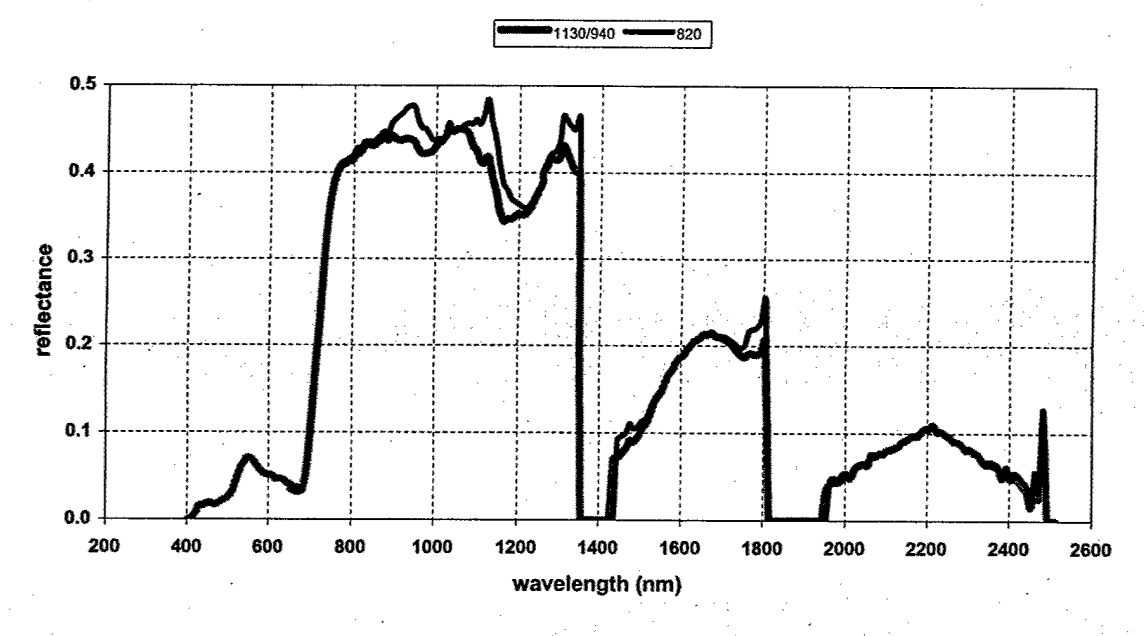


Fig. 4. Grass reflectance spectra retrieved by FLAASH using the 1130 (or 940) and 820 nm regions for water vapor column determination.

In order to help gain a better understanding of the effect of water vapor column amount on the FLAASH retrieved reflectance spectra, retrievals were done for the Fort A.P. Hill cube using three water amounts: 0.1x, 0.4x, and 0.7x the MODTRAN mid-latitude summer profile, which contains 3636 atm-cm of water vapor. Reflectance spectra results are shown in Figs. 5 and 6 for the same two pixels used for Figs. 3 and 4, respectively The 0.4 scale factor yields a column water value approximately the same as was correctly retrieved using either the 1130 or 940 nm absorption band. Thus, the reference (i.e., correct) spectra in Figs. 5 and 6 is the one obtained with the 0.4 water vapor scale factor. The 0.1 and 0.7 scale factors give column values that are 75 % smaller and larger compared to the correct value, respectively. The reflectance spectra in Figs. 5 and 6 obtained using the 0.1 water vapor scale factor contain large valleys (under-correction due to use of a too small water value) at 940 and 1130 nm; as well as, on the wings of the two opaque absorption regions, which are centered near 1400 and 1900 nm. On the other hand, spectra obtained using the 0.7 scale factor contain large spikes (over-correction due to use of a too large water value) at the same wavelength locations of the valleys of the other curve. Each of the two curves containing peaks has a larger one at 1130 nm compared to 940 nm. This is also true of each of the two curves containing valleys. It should be noted that the two curves containing peaks don't have any at 820 nm but the curves are a bit higher than the reference spectra in this wavelength region. Also, the two curves containing valleys don't have any at 820 nm but the curves are a little lower than the reference spectra in this spectral region. These observations show that if the column water vapor value used for the FLAASH reflectance retrieval is incorrect, then the effect is larger at 1130 nm than at 940 nm, while the effect is minimal at 820 nm. This is consistent with the observation that the 1130 nm absorption feature is more sensitive to water vapor than the 940 nm feature and that the 820 nm band only has small sensitivity to water when the true column water vapor value is ~ 1500 nm (see Figs. 1 and 2).

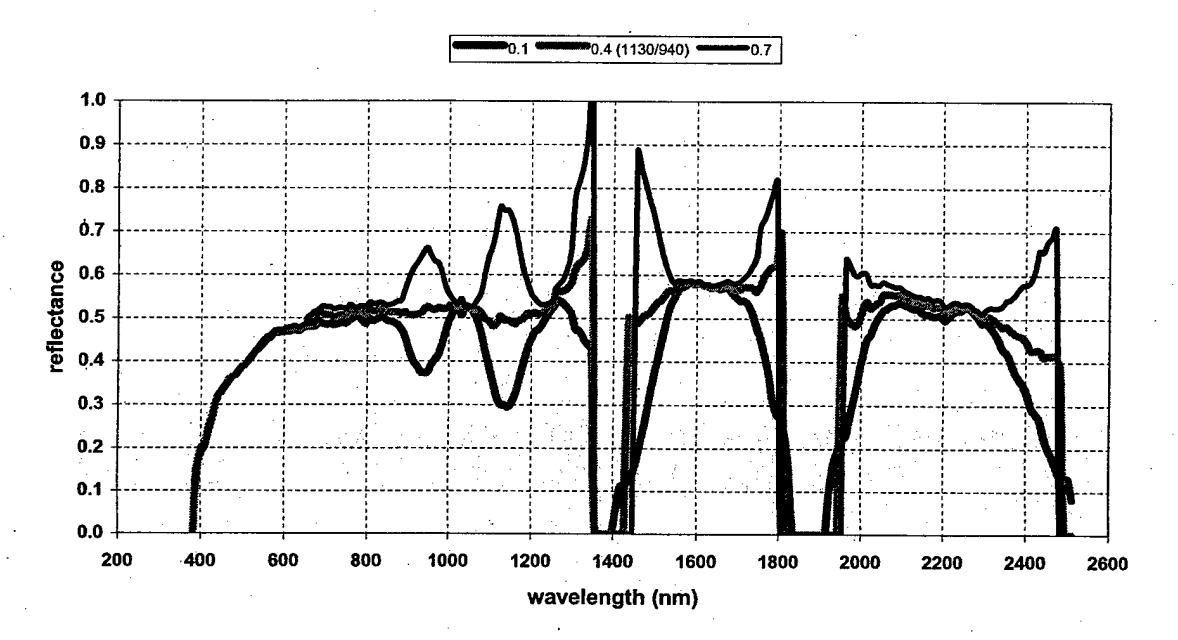


Fig. 5. Building reflectance spectra retrieved by FLAASH using three very different water vapor column amounts.

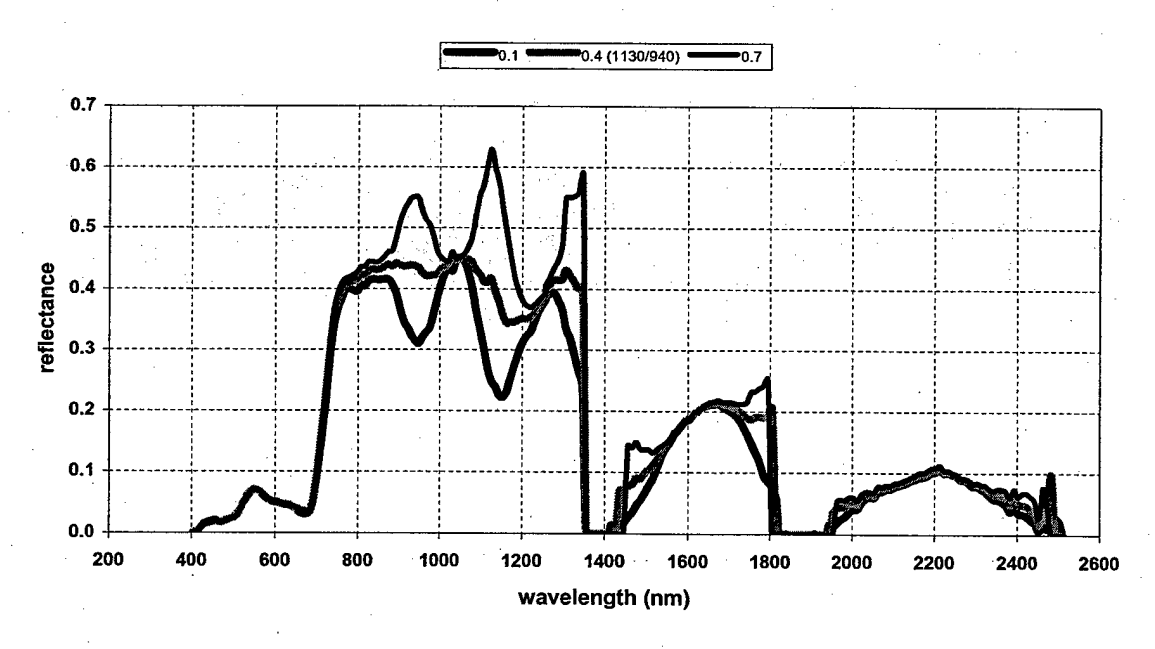


Fig. 6. Grass reflectance spectra retrieved by FLAASH using three very different water vapor column amounts.

5. CONCLUSIONS

FLAASH retrieved column water vapor amounts for three AVIRIS radiance cubes, which were measured under low to moderate moisture conditions (< ~ 4000 atm-cm), are similar using the 1130 or 940 nm absorption region, but are ~ 20 % larger using the 820 nm region. The FLAASH reflectance spectra results for these data cubes using either the 1130 or 940 nm water retrievals are good, but over-correction in the 940 and 1130 nm water vapor absorption regions occurs using the 820 nm water retrievals. These results are consistent with information obtained from a column water vapor sensitivity analysis of MODTRAN calculated radiance values, which shows that the 820 nm band has limited sensitivity, while the 940 and 1130 nm have high sensitivity for low to moderate amounts of water vapor. This analysis also shows for high values of water vapor that the sensitivity is best at 820 nm; however, it is quite low in all three absorption regions. There is a need to examine an expanded set of measured radiance cubes, which cover the complete range of possible moisture conditions, to better quantify the differences in FLAASH water vapor column retrievals using the 820, 940, and 1130 nm regions and also the differences in the corresponding FLAASH retrieved reflectance spectra.

REFERENCES

Ackerman, S.A., K.I. Strabala, W.P. Menzel, R.A. Frey, C.C. Moeller, and L.E. Gumley, "Discriminating Clear Sky from Clouds with MODIS," *J. Geophys. Res.* 103, 32141, 1998.

Adler-Golden, S., A. Berk, L.S. Bernstein, S. Richtsmeier, P.K. Acharya, and M.W. Matthew, G.P. Anderson, C. L. Allred, L.S. Jeong, and J.H. Chetwynd, "A MODTRAN4 Atmospheric Correction Package for Hyperspectral Data Retrievals and Simulations," Summaries of the Seventh JPL Airborne Earth Science Workshop, JPL Publication 97-21, 1, pp. 9-14, 1998.

Anderson, G. P., A. Berk, P. K. Acharya, M. W. Matthew, L. S. Bernstein, J. H. Chetwynd, H. Dothe, S. M. Adler-Golden, A. J. Ratkowski, G. W. Felde, J. A. Gardner, M. L. Hoke, S. C. Richtsmeier, B. Pukall, J. Mello and L. S. Jeong, "MODTRAN4: Radiative Transfer Modeling for Remote Sensing", In *Algorithms for Multispectral, Hyperspectral, and Ultraspectral Imagery VI*, Sylvia S. Chen, Michael R. Descour, Editors, Proceedings of SPIE Vol. 4049, pg. 176-183, 2000.

Berk, A, L.S. Bernstein, D.C. Robertson, P.K. Acharya, G.P. Anderson, and J.H. Chetwynd, "MODTRAN Cloud and Multiple Scattering Upgrades with Application to AVIRIS," Summaries of the Sixth Annual JPL Airborne Earth Science Workshop, JPL Publication 96-4, Vol. 1, Pasadena, California, pp. 1-7, 1996.

Boardman, J.W., "Post-ATREM Polishing of AVIRIS Apparent Reflectance Data using EFFORT: a Lesson in Accuracy versus Precision," Summaries of the Seventh JPL Airborne Earth Science Workshop, JPL Publication 97-21, Vol. 1, p. 53, 1998.

Borel, C.C., P.V. Villeneuve, W.B. Clodius, J.J. Szymanski, and A.B. Davis, "Practical Atmospheric Correction Algorithms for a Multi-spectral Sensor from the Visible through the Thermal Spectral Regions," SPIE '99 Paper, Conf. 3717-19, Los Alamos National Laboratory Report No. LA-UR-99-1374, 1999.

Felde, G.W., G.P. Anderson, T.W. Cooley, M.W. Matthew, S.M. Adler-Golden, A. Berk, and J. Lee, "Anaylsis of Hyperion Data with the FLAASH Atmospheric Correction Algorithm," *Proceedings of the 2003 International Geoscience and Remote Sensing Symposium (IGARSS)*, Toulouse France, 2003.

Kaufman, Y.J., A.E. Wald, L.A. Remer, B.-C. Gao, R.-R. Li and L. Flynn, "The MODIS 2.1-micron Channel - Correlation with Visible Reflectance for Use in Remote Sensing of Aerosol," *IEEE Trans. Geosci. Remote Sensing*, V35, 1286-1298, 1997.

Matthew, M. W., S. M. Adler-Golden, A. Berk, S. C. Richtsmeier, R.Y. Levine, L. S. Bernstein, P. K. Acharya, G. P. Anderson, G. W. Felde, M. L. Hoke, A. J. Ratkowski, H.-H. Burke, D. Miller J. H. Chetwynd, "Status of Atmospheric Correction Using a MODTRAN4-based Algorithm," In *Algorithms for Multispectral, Hyperspectral, and Ultraspectral Imagery VI*, Sylvia S. Chen, Michael R. Descour, Editors, Proceedings of SPIE Vol. 4049, pg. 207, 2000.

Staenz, K., D.J. Williams, and B. Walker, "Surface Reflectance Retrieval from AVIRIS Data Using a Six-Dimensional Look-Up Table," *Summaries of the Sixth Annual JPL Airborne Earth Science Workshop*, March 4-8, 1996, JPL Publication 96-4, Vol. 1, Pasadena, California, pp. 223-229, 1996.

Vermote, E., D. Tanre, J.L. Deuze, M. Herman, and J.J. Morcrette, "Second Simulation of the Satellite Signal in the Solar Spectrum (6S)," 6S User Guide Version 6.0, NASA-GSFC, Greenbelt, Maryland, 134 pages, 1994.